

Transition of phase locking modes in a minimal neuronal network

Qingyun Wang^{a,*}, Miguel A.F. Sanjuán^b, Guanrong Chen^c

^a Department of Dynamics and Control, Beihang University, Beijing 100191, China

^b Departamento de Física, Universidad Rey Juan Carlos, Tulipán s/n, 28933 Móstoles, Madrid, Spain

^c Department of Electronic Engineering, City University of Hong Kong, Hong Kong SAR, China

ARTICLE INFO

Article history:

Received 13 July 2011

Received in revised form

9 October 2011

Accepted 13 November 2011

Communicated by J. Cao

Available online 26 December 2011

Keywords:

Phase locking

Inhibitory synapse

Excitatory synapse

Phase plane analysis

ABSTRACT

We investigate the dynamics of phase locking in a minimal neuronal network, which is composed of two Morris–Lecar neurons that are coupled by inhibitory and excitatory synapses as the synaptic strength is varied. Studies show that the synaptic strength can induce various phase locking modes and complex chaotic behaviors. In particular, two coupled neurons may display the complicated transitions between various periodic phase locking modes and chaotic states. It is shown that those transitions are accompanied by the tangent bifurcation, where the different phase locking modes can be related to the appearance of periodic windows. Furthermore, we explore the dynamical mechanism of the phase locking modes by means of the phase plane analysis. Interestingly, we have found two types of 2:1 phase locking modes, which are characterized by a thin tadpole tail and a fat tadpole tail, respectively. And then, two types of 2:1 phase locking modes are analyzed in detail for understanding their dynamical mechanism. The obtained results can be helpful to explore realistic neuronal activities.

© 2011 Elsevier B.V. All rights reserved.

1. Introduction

Synchronous firing activity in the cortical network is thought to be the basis of complex dynamical behaviors, which are related to memory such as word recollection [1] and facial recognition [2]. It has also been suggested as particularly relevant for the efficient processing and transmission of neuronal signals [3–6]. Neuronal synchronization on complex networks has been explored in detail [7–12,14,15], leading to several insights that have the potential of applicability on realistic problems in neurosciences. In particular, for fully connected networks of identical neurons of purely excitatory interactions, synchronization properties are analyzed by considering their dependence on the time course of the synaptic interaction and on the response of the neurons to small depolarization [13]. The influence of the coupling strength and network topology on synchronization was studied for networks of bursting Hindmarsh–Rose neurons coupled by chemical synapses in Ref. [14]. Furthermore, Batista et al. [16,17] have studied the onset of phase synchronization on scale-free bursting neurons networks. Interestingly, it was reported that chemical and electrical synapses perform complementary roles in the synchronization of interneuronal networks [15]. In addition, based on the theory of stochastic phase dynamics, Wang et al. investigated the neural phase motion and neural coding of population and found

some new characteristics of neurodynamics [18–20]. The interesting result shows that the variable coupling mechanism can induce the transition of different cluster states and synchronization of the neuronal oscillator population [21–23].

Recently, synchronization and its related transition process of neuronal networks with time delay have received considerable attention as some key parameters vary. For example, we have found that the information transmission delay can induce synchronization transitions in a scale-free neuronal network [24–26], where both gap junction and chemical coupling are considered, respectively. The synchronized behaviors of a noisy small-world neuronal network with delay and diversity are numerically studied, and it is shown that a delay can induce fruitful synchronization transitions from phase locking to antiphase synchronization, and a transition from antiphase synchronization to complete synchronization [27]. Also, Liang et al. [28] has analyzed the effects of distributed delays on phase synchronization of bursting neurons, where it was found that a time delay can change the state of the excitable system from a predominantly spiking behavior to a largely bursting behavior. In sum, the delay can generate complex dynamics and many interesting and even unexpected phenomena [24–31].

In order to better understand the complex dynamics of large scale neuronal networks, it would be important to investigate the behavior of a minimal neuronal network, which is composed of two neurons. When the coupling between oscillators is weak, synchronization and its stability in a homogeneous two-cell network can be analyzed using the well-developed geometric

* Corresponding author. Tel./fax: +86 10 82332003.
E-mail address: nmqingyun@163.com (Q. Wang).

phase-reduction approach and the method of averaging [32–34]. The loss of synchrony caused by an increase in inhibitory coupling in networks of type-I Morris–Lecar model oscillators has been reported, in which a period-doubling cascade to mode-locked states with alternation is found in the firing order of the two cells [35,36]. Functional phase response curves are proposed to allow the prediction of phase locking, even in cases of strong coupling with a significant adaptation in a network consisting of two single compartment WB model neurons [37].

However, in spite of the many works on neuronal synchronization done in past several decades, we are still far away from a real understanding of neuronal information processing and complex dynamic behaviors of brain networks. Here, we aim to extend previous studies on this topic by considering a minimal neuronal network, which is composed of two Morris–Lecar neurons coupled by an inhibitory and an excitatory synaptic interaction. We mainly focus on dynamic transitions of the neuronal network as the synaptic parameter varies. Results show that various phase locking modes and complex chaotic states can appear in this minimal neuronal network. A phase locking mode can be identified by the routes from chaos to the periodic window when the synaptic strength is varied. More interestingly, we find two types of 2:1 phase locking modes with a thin tadpole tail and a fat tadpole tail. Furthermore, the phase locking modes are analyzed in detail from the phase plane dynamics.

The remainder of this paper is organized as follows. In the next section we introduce the mathematical model of the neuronal network. The main results are presented in Section 3, whereas the last section summarizes the new findings.

2. Mathematical model and setup

As a minimal neuronal network, we investigate the dynamics of two coupled Morris–Lecar (ML) neurons [38] with excitatory and inhibitory synapses. The coupled configuration is shown in Fig. 1. The resulting dynamical equations are described as follows:

$$C \frac{dV_I}{dt} = -I_{Ca} - I_K - I_L - I_{syn}^{E,I} - I_{app} \quad (1)$$

$$\frac{d\omega_I}{dt} = \frac{(\omega_\infty - \omega_I)}{\tau_\infty(V_I)} \quad (2)$$

$$C \frac{dV_E}{dt} = -I_{Ca} - I_K - I_L - I_{syn}^{I,E} - I_{app} \quad (3)$$

$$\frac{d\omega_E}{dt} = \frac{(\omega_\infty - \omega_E)}{\tau_\infty(V_E)} \quad (4)$$

$$I_{Ca} = g_{Ca} m_\infty(V_i)(V_i - V_{Ca}) \quad (5)$$

$$I_K = g_K \omega(V_i)(V_i - V_K) \quad (6)$$

$$I_L = g_L(V_i - V_L) \quad (7)$$

where V_i (i stands for I or E) is the neuron membrane potential in mV, I_{Ca} is the depolarizing calcium current, and I_L is the passive

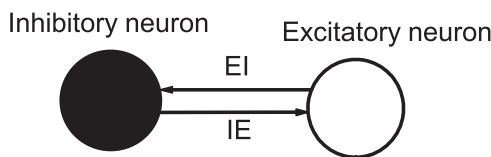


Fig. 1. Schematic presentation of the connectivity between two neurons, where two neurons interact through excitatory and inhibitory synapses, respectively. EI (IE) denotes the effect of excitatory (inhibitory) neuron on the inhibitory (excitatory) neuron through chemical synapses.

leak current, respectively. Moreover, $\omega_{I,E}$ is the activation of the repolarizing potassium current I_K , t is the time in ms, and $I_{app} = -14 \mu\text{A}/\text{cm}^2$ is the applied current. The remaining parameters are fixed as $V_{Ca} = 120 \text{ mV}$, $V_K = -84 \text{ mV}$, $V_L = -60 \text{ mV}$, $g_{Ca} = 4 \text{ mS}/\text{cm}^2$, $g_K = 8 \text{ mS}/\text{cm}^2$, and $g_L = 2 \text{ mS}/\text{cm}^2$.

The steady state activation of the calcium current is

$$m_\infty(V) = \frac{1}{2} \left[1 + \tanh \left(\frac{V+12}{18} \right) \right] \quad (8)$$

The potassium current activation amplitude and activation rate are given as follows, respectively,

$$\omega_\infty(V) = \frac{1}{2} \left[1 + \tanh \left(\frac{V+8}{6} \right) \right] \quad (9)$$

$$\frac{1}{\tau_\infty(V)} = \frac{2}{3} \cosh \left(\frac{V+12}{18} \right) \quad (10)$$

The two neurons are coupled through the synaptic current given by

$$I_{syn}^{i,j} = -g_{syn}^i s_j(t)(V_i - V_{inh(exc)}) \quad (11)$$

where g_{syn} is the strength of synaptic conductance, and $V_{inh} = -80 \text{ mV}$ and $V_{exc} = 20 \text{ mV}$ are the reversal potential for inhibitory and excitatory synapses, respectively. The dynamics of the synaptic gating variable $s(t)$ depends on the presynaptic neuron potential, V_i

$$\frac{ds_j}{dt} = -\frac{s_j}{\tau_{syn}} \sigma(V_{th} - V_i) + \frac{1-s}{\tau_\gamma} \sigma(V_i - V_{th}) \quad (12)$$

where $V_{th} = -3 \text{ mV}$ is the synaptic threshold, σ is a sigmoid function, and $\sigma(x) = (1 + \tanh(4x))/2$. $\tau_{syn} = 1.0$ and $\tau_\gamma = 0.2 \text{ ms}$ are the synaptic decay and rising time constants, respectively. Note that for this choice of model parameters, each of the two uncoupled ML neurons exhibits periodic spiking.

3. Results

3.1. Transition of phase locking modes

For this minimal neuronal network, we firstly investigate in detail the dynamical behavior of the two identical ML model neurons, which are coupled by inhibitory and excitatory synapses as described by above Eqs. (1)–(12). Fig. 2 shows bifurcation diagrams of inter-spike intervals (ISIs) of the inhibitory (I) neuron, excitatory (E) neuron and coupled neuronal network, respectively as the synaptic strength g_{syn} increases. Here, as noted in Ref. [35], ISIs of the coupled network are recorded as the asymptotic intervals between two consecutive spikes of the neuronal network, which may or may not be the spikes of the same neuron. And then, they are normalized to the period of the uncoupled neuron, and are denoted as ISI_{norm} . It is clear in Fig. 2 that as the synaptic strength g_{syn} is relatively small, two neurons exhibit nearly periodic synchronization behavior with a small deviation of their phases. As g_{syn} is increased, two neurons begin to slide into non-periodic motion, and the behavior of the neuronal network becomes chaotic. For further increasing synaptic strength, the periodic window can intermittently appear via the tangent bifurcation as shown in Figs. 2 and 3. For more detailed investigations, the chaotic behavior and periodic motions can intermittently transit as the synaptic strength increases. Hence, we can observe complex transition modes in two coupled ML neurons with inhibitory and excitatory synapses as the synaptic strength g_{syn} varies. In particular, as shown in Fig. 2, we have labeled some typical positions A, B, C, and D, where different periodic windows can be exhibited. In fact, the periodic windows

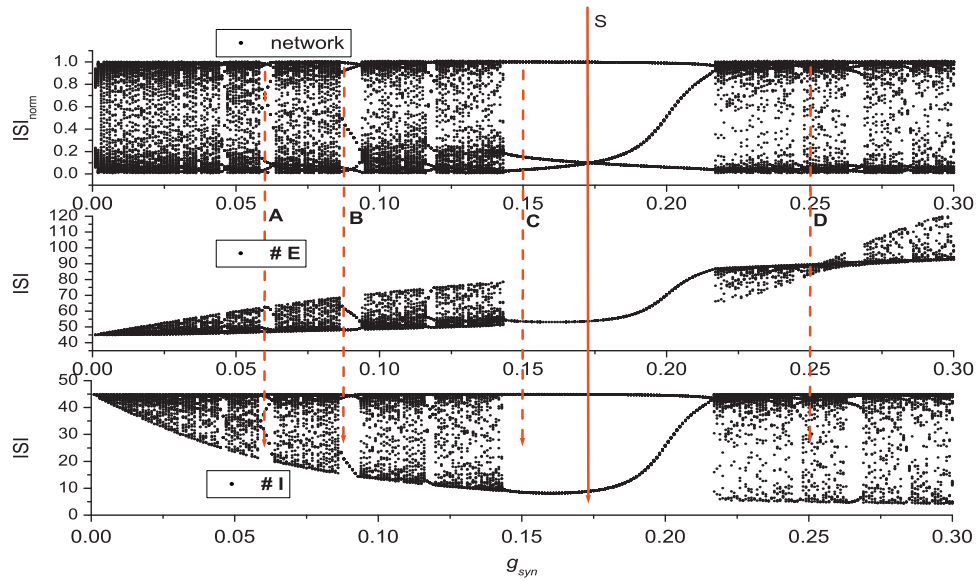


Fig. 2. From the bottom to top, the bifurcation diagrams of inter-spike intervals (ISIs) of I neuron, E neuron and the coupled neuronal network are shown as the synaptic strength g_{syn} is increased. Note that ISIs of the coupled network are recorded as the asymptotic intervals between two consecutive network spikes, which may or may not be the spikes of the same neuron. And then they are normalized to the period of the uncoupled neuron, and are denoted as ISI_{norm} .

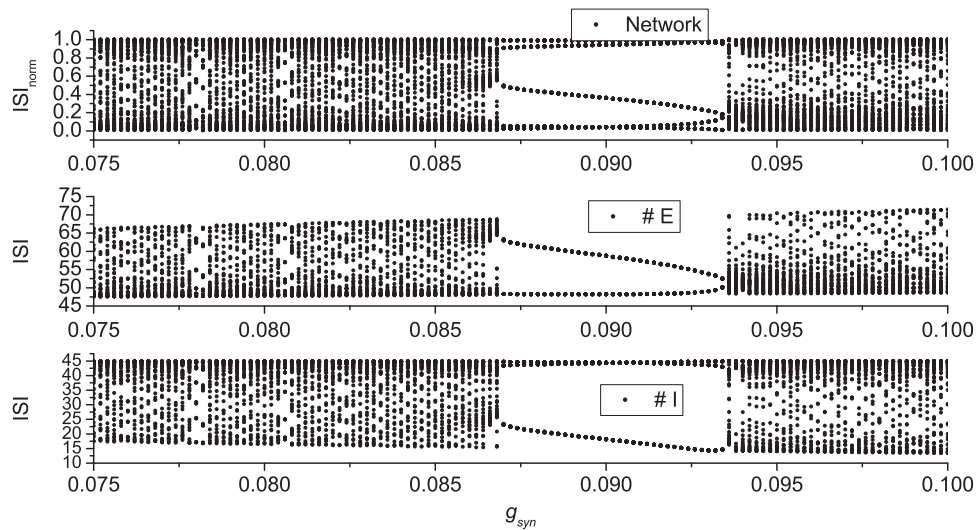


Fig. 3. An enlargement of Fig. 2, which clearly shows the occurrence of a 3:2 phase locking mode, where an I neuron can spike three times and an E neuron fires twice.

correspond to different phase locking modes. As an example, a local enlargement part of Fig. 2 is shown in Fig. 3, where it can clearly be observed that a 3:2 phase locking mode can be clearly exhibited. Hence, it is inferred that different phase locking transitions can be identified via the bifurcation diagram of ISIs as the synaptic strength increases.

In order to supplement the visual assessment of bifurcation diagrams presented in Fig. 2, we will examine the time series of membrane potentials of the coupled neurons, which can intuitively guide us to determine how two neurons lock between their phases, for some typical values of synaptic strength g_{syn} . In particular, Fig. 4(a) shows a 4:3 phase locking mode between two neurons as the synaptic strength $g_{syn} = 0.062$. If the synaptic strength is increased to $g_{syn} = 0.09$, a 3:2 phase locking mode can appear as shown in Fig. 4(b). Further increasing synaptic strength can lead to a 2:1 phase locking mode (see Fig. 4(c)). However, chaotic patterns can occur when one type of the phase lockings transits to another type of them. For example, as the synaptic strength is increased to $g_{syn} = 0.25$, the coupled network can

exhibit chaotic behavior and two neurons look like non-periodic (see Fig. 4(d)). Hence, it can be concluded that for the coupled two ML neurons with inhibitory and excitatory synapses, the various phase locking modes and complex chaotic states can be intermittently exhibited as the synaptic strength g_{syn} varies.

3.2. Dynamic analysis of phase locking modes

In what follows, it remains interesting to provide a simple geometric explanation and quantitative analysis for different phase locking modes. To do this, it is crucial to understand the difference for the effects of excitatory and inhibitory stimuli on the phase plane dynamics of a single ML neuron. Based on the phase plane analysis, Fig. 5 illustrates schematically the effect of the presynaptic neuron on the dynamics of the post-synaptic one. This idea is proposed by Oh et al. [35], and it can well capture the frog-leap solutions and alternative firing order of two ML neurons coupled by the inhibitory synapses. In particular, it is shown in Fig. 5(a) that there is no qualitative change in the geometry for a

wide range of excitatory effects, where the V -nullcline and the ω -nullcline intersect at the middle branch with only one point. However, as illustrated in Fig. 5(b), an obvious qualitative change can occur when the inhibitory synapse becomes sufficiently strong, which can suppress the neuron below its excitation through the saddle-node on the invariant cycle bifurcation [34]. As a result, there are three points, where the V -nullcline and the ω -nullcline can intersect. Clearly, as shown in Fig. 5(b), the red point below the excitation is very important for our understanding of the phase locking modes. On one hand, the suitable inhibitory coupling results in a transient subthreshold trapping of one neuron during each cycle of the oscillation, and the neuron is delayed for spiking. Consequently, the neuron can bypass its partner neuron along the limit cycle by transiently keeping the

other inhibited neuron in the subthreshold tadpole tail branch of the trajectory, as depicted in Fig. 5(b). On the other hand, the excitatory effects can lead to more frequent spiking during the given time interval. Hence, various phase locking modes can appear as long as the interactions of inhibitory and excitatory neurons are exactly chosen.

As a typical case, we investigate the 2:1 phase locking mode from the phase plane dynamics of the coupled system. Firstly, the time series of membrane potentials of two coupled neurons are illustrated in Fig. 6 as the synaptic strength $g_{syn} = 0.15$ and $g_{syn} = 0.2$, respectively. It is obvious that both Fig. 6(a) and (b) shows the 2:1 phase locking of the coupled ML neurons. However, we can find that the two types of phase locking are a bit different. Comparing Fig. 6(a) with (b), it is clear that for $g_{syn} = 0.2$, the excitatory neuron has longer silent state than the case of synaptic strength $g_{syn} = 0.15$. In fact, this results from the larger and more suitable synaptic strength, which delays the next spike of excitatory neuron by the inhibitory neuron. From the above analysis, as shown in Fig. 5, more detailed differences can be explained when one considers the phase plane dynamics of the coupled neuronal systems. Here, we denote the inhibitory neuron and excitatory one as the filled black and open red circles. For the synaptic strength $g_{syn} = 0.15$, it is shown in Fig. 6(a) that the black neuron initially spikes, and the red neuron stays in a silent state and is slowly heading for spiking. When the red neuron spikes, which pushes the black neuron into the subthreshold branch of the trajectory. When the red neuron jumps down and stays below the excitation threshold and off the limit cycle trajectory, which forms a tadpole tail as shown in Fig. 6, the black neuron begins to leave the subthreshold branch of the trajectory. As the time evolves, the black neuron spikes and the red neuron is still trapped into the tadpole tail. Next, the black neuron jumps into another region of the subthreshold region (see Fig. 7(e)). Finally, the black neuron bypasses the red neuron along the unperturbed limit cycle trajectory and spikes again. At the same time, the red neuron also escapes the tadpole tail and is heading for the next spiking due to the inhibitory effects of the black neuron, which drops its V nullcline. Hence, the sequence of six panels describes the dynamical mechanism of the 2:1 phase locking mode.

Interestingly, we will explore another 2:1 phase locking mode as shown in Fig. 6(b). Similarly, we capture some typical positions

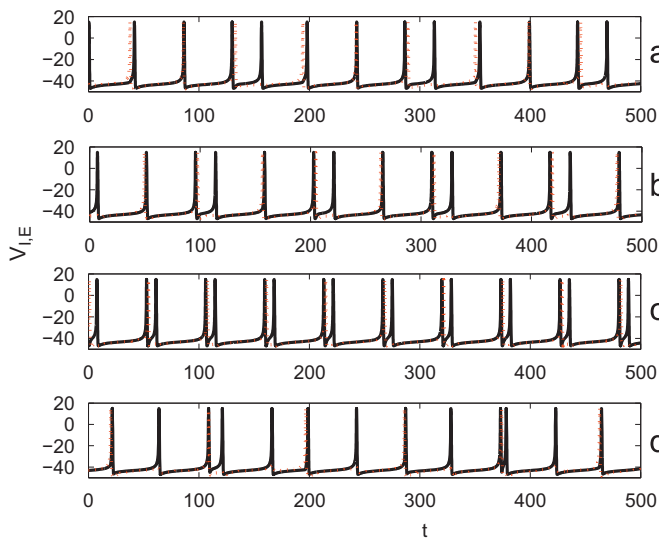


Fig. 4. Phase locking state of the two coupled neurons at different values of synaptic strength g_{syn} . The membrane potentials of the two neurons are shown as black solid line (I neuron) and red dash line (E neuron), respectively. (a) 4:3 phase-locked firing ($g_{syn} = 0.062$). (b) 3:2 phase-locked firing ($g_{syn} = 0.09$). (c) 2:1 phase-locked firing ($g_{syn} = 0.15$). (d) Chaotic state, irregular inter-spike intervals ($g_{syn} = 0.25$). (For interpretation of the references to color in this figure legend, the reader is referred to the web version of this article.)

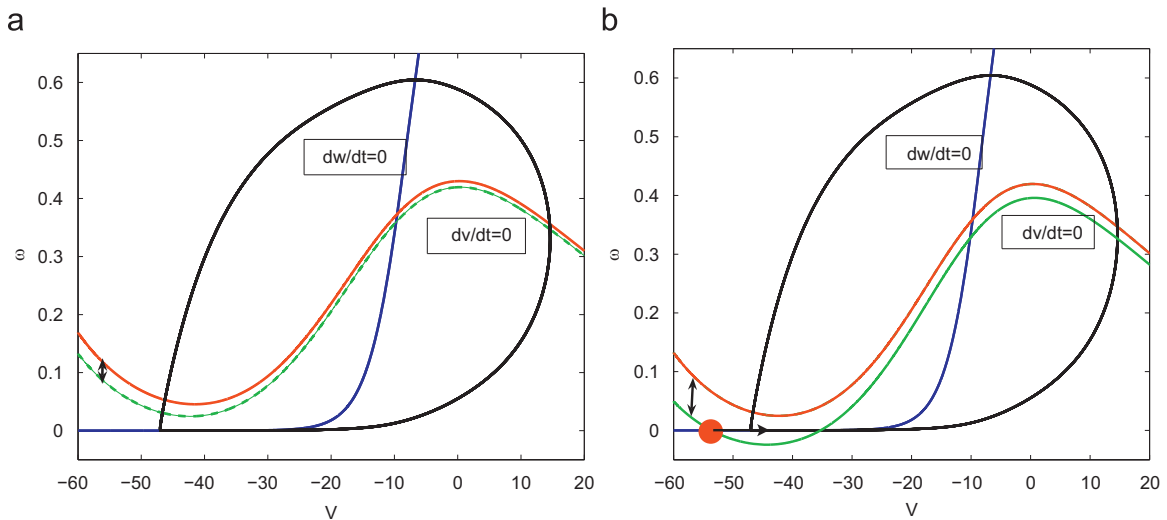


Fig. 5. Effect of the coupling on the phase-plane trajectory of the postsynaptic neuron. Double arrows indicate the movement of the V -nullcline during each cycle of the neuron. (a) In the case of excitatory effect, an increase in synaptic coupling causes no qualitative change in the phase-plane dynamics. (b) For sufficiently strong inhibitory effect, the V -nullcline of the postsynaptic neuron intersects the ω -nullcline with each presynaptic input, pushing the neuron below the excitation threshold and off the limit cycle trajectory, which forms a tadpole tail. Here, red dot denotes the neuron trapped in the tadpole tail. (For interpretation of the references to color in this figure legend, the reader is referred to the web version of this article.)

of two neurons in the phase plane. As shown in Fig. 7, the sequence of six panels describes the leap-frog spike sequence of the two coupled neurons as shown in Fig. 6(b). Initially, the black neuron spikes and the red one stays in a silent state (see Fig. 7(a)). Thus, it can be found in Fig. 7(b) that when the black neuron jumps down into one subthreshold region, the red neuron still stays in a silent state, and then, the red neuron spikes. When the red neuron is jumping down, the black neuron spikes again, pushing the red neuron into the subthreshold branch of the trajectory. As a result, the red neuron jumps into the tadpole tail and the black neuron bypasses the red neuron along the

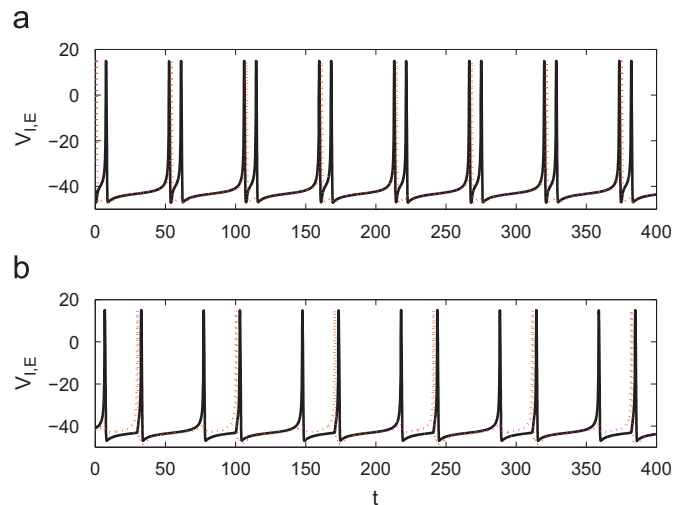


Fig. 6. Transition of the 2:1 phase-locked firing. (a) $g_{syn}=0.15$. (b) $g_{syn}=0.2$. (For interpretation of the references to color in this figure legend, the reader is referred to the web version of this article.)

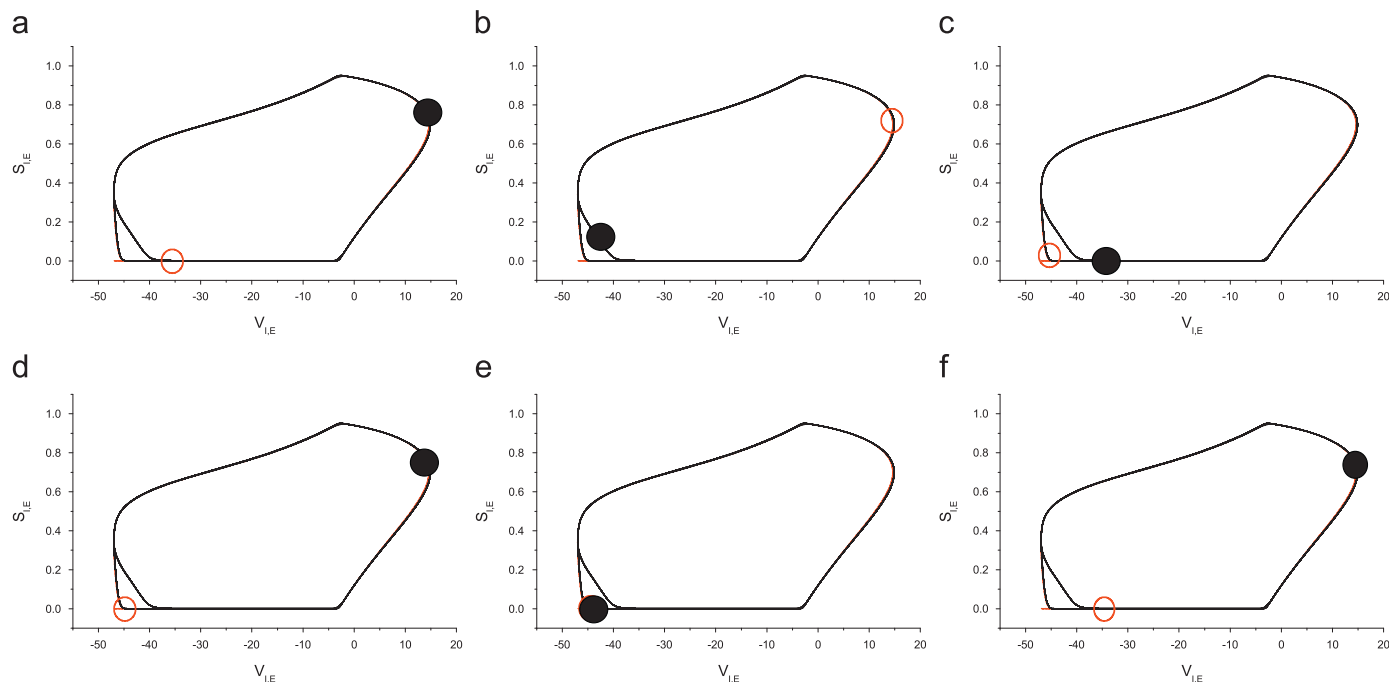


Fig. 7. Phase-plane dynamics of the coupled Morris–Lécar neurons during the 2:1 phase-locked firing. The sequence of six panels describes the leap-frog spike sequence as shown in Fig. 5(a) with filled black and open red circles representing the two neurons; (a) black neuron spikes; (b) red neuron spikes, pushing the black neuron into the subthreshold branch of the trajectory; (c) red neuron jumps into thin tadpole tail and black neuron bypasses the red neuron along the unperturbed limit cycle trajectory; (d) black neuron spikes again and red neuron always stay in tadpole tail; (e) black neuron jumps into another region of subthreshold, and leave it for the next spiking; (f) black neuron spikes again, and the process then repeats itself, with the red neuron emitting the next spike. (For interpretation of the references to color in this figure legend, the reader is referred to the web version of this article.)

unperturbed limit cycle trajectory with outer circle. After some time, the black neuron spikes again, and the process then repeats itself.

By comparing Figs. 7 and 8, very interesting results in the network we are considering can be found, in particular we can find that the formation of the phase locking mode is different between them. Thus, it is obvious that for the red neuron inhibited by the black neuron, the formed tadpole tails between them are a bit different. We call formally them as thin tadpole tail (see Fig. 7) and fat tadpole tail (see Fig. 8), respectively. Enlargements of the corresponding figures are in Fig. 9(a) and (b), respectively, which can clearly guide our visions to identify different tadpole tails. In fact, it is understandable that for a stronger inhibition, the frog-leap can occur more slowly. And then, there appears a fat tadpole tail in Fig. 8. In addition, from Fig. 9(a) and (b), it is more intuitive to understand the generation mechanism of two types of 2:1 phase locking modes in the analyzed network. In particular, for the thin tadpole tail mode, there exists a big gap between two subthreshold regions of the black neuron, and there is a very narrow gap between the outer circle of the black neuron and the region below the excitation of the red neuron. Thus, for the fat tadpole tail mode, the opposite is true.

4. Summary and discussion

In summary, we have analyzed the phase locking modes and complex chaotic states in a minimal neuronal network, which is composed of two ML neurons that are coupled with inhibitory and excitatory synapses. It is shown that as the synaptic strength varies, various periodic phase locking can be exhibited in the neuronal network under this investigation. In addition, we can find that transitions among different phase locking modes are accompanied by chaotic states. Furthermore, based on a phase

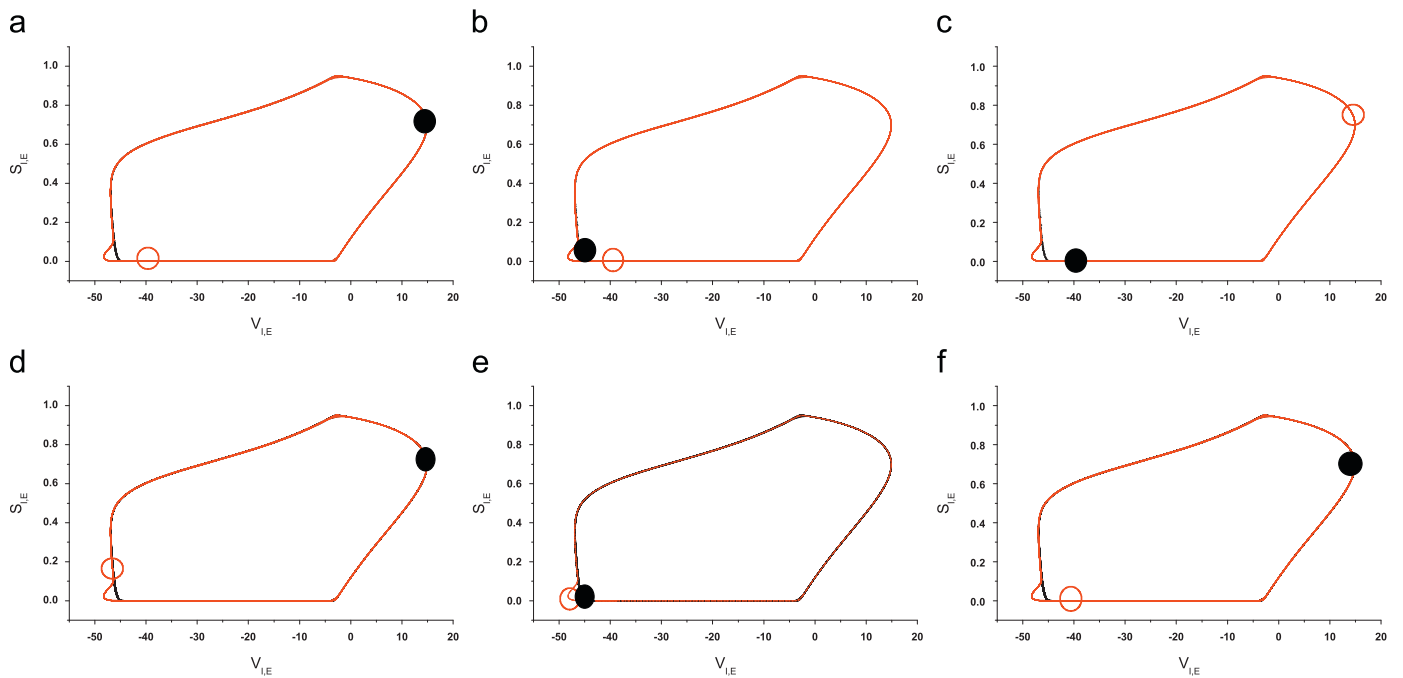


Fig. 8. Phase-plane dynamics of the coupled Morris–Lecar model neurons during the 2:1 phase-locked firing. The sequence of six panels describes the leap-frog spike sequence as shown in Fig. 5(b), with filled black and open red circles representing the two neurons: (a) black neuron spikes; (b) black neuron jumps into subthreshold region, and red neuron still stays in a silent state; (c) red neuron spikes (d) black neuron spikes again, pushing the red neuron into the subthreshold branch of the trajectory; (e) red neuron jumps into tadpole tail and black neuron bypasses the red neuron along the unperturbed limit cycle trajectory; (f) black neuron spikes again, and the process then repeats itself, with the red neuron emitting the next spike. (For interpretation of the references to color in this figure legend, the reader is referred to the web version of this article.)

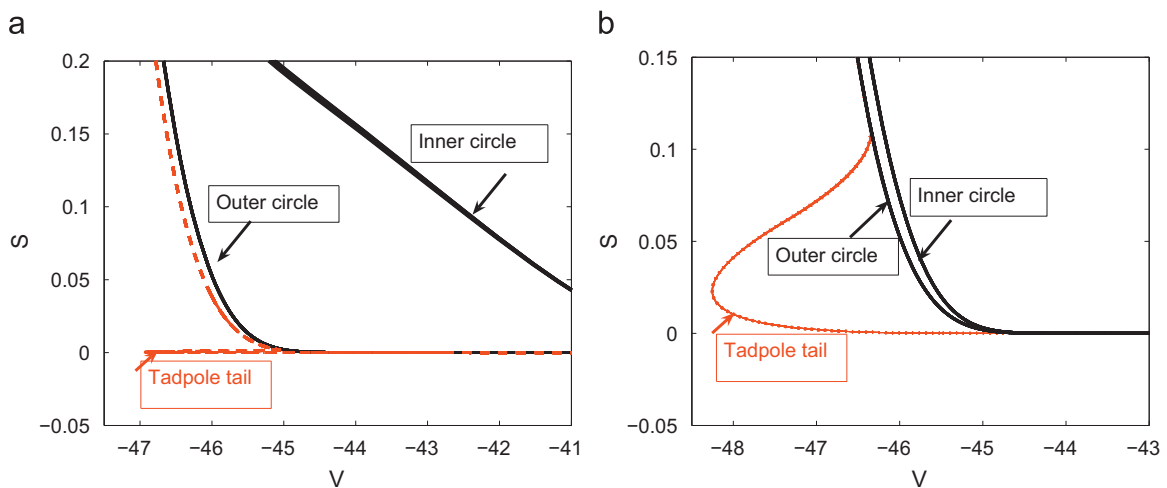


Fig. 9. The enlargement of Figs. 7 and 8, which shows the subthreshold motion of two neurons. For $g_{syn} = 0.15$, the tadpole of the red neuron is thin and black neuron has two subthreshold regions, which is distant enough. For $g_{syn} = 0.15$, the tadpole of the red neuron is fat and black neuron has two subthreshold regions, which is very close. These regions can guide us to understand two types of a 2:1 phase locking modes. (For interpretation of the references to color in this figure legend, the reader is referred to the web version of this article.)

plane dynamical analysis, the dynamical mechanism of phase locking modes is investigated in detail. Interestingly, we have found two types of 2:1 phase locking modes, which are termed as the thin tadpole tail and fat tadpole tail, respectively. Furthermore, the dynamics of two types of 2:1 phase locking modes are explored. It is shown that inhibitory and excitatory GABA connections can coexist in the cerebellar interneuron network. Studies have suggested also that the coexistence of excitatory and inhibitory GABA synapses could either buffer the mean firing rate of the interneuron network or introduce different types of correlation between neighboring interneurons, or both [39].

Hence, we hope that our study might be useful for understanding real neuronal activity, especially for investigating collective behaviors of large scale neuronal networks.

Acknowledgments

This work was supported by the National Science Foundation of China under Project Nos. 11172017, 10972001 and 10832006. MAFS acknowledges financial support from the Spanish Ministry of Science and Innovation under Project No. FIS2009-09898.

References

- [1] J. Fell, P. Klaver, K. Lehnertz, T. Grunwald, C. Schaller, C.E. Elger, et al., *Nat. Neurosci.* 4 (12) (2001) 1259–1264.
- [2] E. Rodriguez, N. George, J.P. Lachaux, J. Martinerie, B. Renault, F.J. Varela, *Nature* 397 (6718) (1999) 430–433.
- [3] J.A.K. Suykens, G.V. Osipov, *Chaos* 18 (2008) 037101.
- [4] T. Nowotny, R. Huerta, M.I. Rabinovich, *Chaos* 18 (2008) 037119.
- [5] C.M. Gray, W. Singer, *Proc. Natl. Acad. Sci. USA* 86 (1989) 1698.
- [6] M. Bazhenov, M. Stopfer, M. Rabinovich, R. Huerta, H.D.I. Abarbanel, T.J. Sejnowski, G. Laurent, *Neuron* 30 (2001) 553.
- [7] D.-S. Lee, *Phys. Rev. E* 72 (2005) 026208.
- [8] A.E. Motter, C.S. Zhou, J. Kurths, *Europhys. Lett.* 69 (2005) 334.
- [9] C. Zhou, J. Kurths, *Phys. Rev. Lett.* 96 (2006) 164102.
- [10] A. Arenas, A. Diaz-Guilera, C.J. Perez-Vicente, *Physica D* 224 (2006) 27.
- [11] Q.Y. Wang, Q.S. Lu, G.R. Chen, D.H. Guo, *Phys. Lett. A* 356 (2006) 17.
- [12] T. Kunichika, Y. Tetsuya, A. Kazuyuki, K. Hiroshi, *Int. J. Bifurcation Chaos* 13 (2003) 653.
- [13] D. Hansel, G. Mato, C. Meunier, *Neural Comput.* 7 (1995) 307.
- [14] I. Belykh, E. de Lange, M. Hasler, *Phys. Rev. Lett.* 94 (2005) 188101.
- [15] N. Kopell, B. Ermentrout, *Proc. Natl. Acad. Sci. USA* 101 (2004) 15482.
- [16] C.A.S. Batista, A.M. Batista, J.A.C. de Pontes, R.L. Viana, S.R. Lopes, *Phys. Rev. E* 76 (2007) 16218.
- [17] C.A.S. Batista, A.M. Batista, J.A.C. de Pontes, S.R. Lopes, R.L. Viana, *Chaos Solitons Fractals* 41 (2009) 2220.
- [18] R.B. Wang, Z.K. Zhang, J.Y. Qu, J.T. Cao, *IEEE Trans. Neural Networks* 22 (7) (2011) 1097.
- [19] Y. Liu, R.B. Wang, Z.K. Zhang, X.F. Jiao, *Cognitive Neurodyn.* 4 (1) (2010) 61.
- [20] R.B. Wang, Z.K. Zhang, C.K. Tse, *Appl. Math. Mech.* 30 (11) (2009) 1415.
- [21] X.D. Zhang, R.B. Wang, Z.K. Zhang, J.Y. Qu, J.T. Cao, X.F. Jiao, *Neurocomputing* 73 (2010) 2665.
- [22] R.B. Wang, X.F. Jiao, *Neurocomputing* 69 (2006) 778.
- [23] X.F. Jiao, R.B. Wang, *Appl. Phys. Lett.* 88 (20) (2006) 203901.
- [24] Q.Y. Wang, M. Perc, Z.S. Duan, G.R. Chen, *Phys. Rev. E* 80 (2) (2009) 026206.
- [25] Q.Y. Wang, G.R. Chen, *Chaos* 21 (1) (2011) 013123.
- [26] Q.Y. Wang, G.R. Chen, M. Perc, *PLoS One* 6 (1) (2011) 0015851.
- [27] J. Tang, J. Ma, M. Yi, H. Xia, X.Q. Yang, *Phys. Rev. E* 83 (2011) 046207.
- [28] X.M. Liang, M. Tang, M. Dhamala, Z.H. Liu, *Phys. Rev. E* 80 (2009) 066202.
- [29] Q.Y. Wang, Q.S. Lu, *Chin. Phys. Lett.* 3 (2005) 543.
- [30] E. Rossoni, Y.H. Chen, M.Z. Ding, J.F. Feng, *Phys. Rev. E* 71 (2005) 061904.
- [31] Q. Wang, Z. Duan, M. Perc, G. Chen, *Europhys. Lett.* 78 (2008) 50008.
- [32] G.B. Ermentrout, N. Kopell, *SIAM J. Math. Anal.* 15 (1984) 215–237.
- [33] E.M. Izhikevich, Y. Kuramoto, *Encyclopedia Math. Phys.* 5 (2006) 448.
- [34] F.C. Hoppensteadt, E.M. Izhikevich, *Weakly Connected Neural Networks*, Springer, New York, 1997.
- [35] M. Oh, V. Matveev, *J. Comput. Neurosci.* 26 (2009) 303.
- [36] S. Achuthan, C.C. Canavier, *J. Neurosci.* 29 (2009) 5218.
- [37] J.X. Cui, C.C. Canavier, R.J. Butera, *J. Neurophysiol.* 102 (2009) 387–398.
- [38] C. Morris, H. Lecar, *Biophys. J.* 35 (1981) 193–213.
- [39] J. Chavas, A. Marty, *J. Neurosci.* 23 (6) (2003) 2019–2031.



Qingyun Wang received the M.Sc. degree in mathematics from Inner Mongolia University, Hohhot, China in 2003 and the Ph.D. degree in general mechanics from Beihang University, Beijing, China in 2006. Between 2008 and 2010, he was a Full Professor at Inner Mongolia Finance and Economics College, Hohhot, China. He is a Full Professor with the Department of Dynamics and Control, Beihang University, Beijing, China since June 2010. His research interests include neuronal dynamics modeling and analysis, dynamics and control of complex networks and the applications of nonlinear dynamics to mechanical and physical systems.



Miguel A.F. Sanjuán received his Degree in Physics from University of Valladolid, Spain in 1981, and a Ph.D. Degree in Physics from National University at a Distance, Madrid, Spain in 1990. He was Visiting Research Associate at the Institute of Physical Science and Technology, University of Maryland, from July 1995 to September 1996 under the supervision of Prof. James A. Yorke. He is a JSPS fellow and he was a Visiting Researcher at the University of Tokyo in February 2002, working in collaboration with Prof. Kazuyuki Aihara. Since 2002 he is Full Professor of Physics at the University Rey Juan Carlos, Madrid, Spain, where he is the Head of the Department of

Physics and the Head of the Nonlinear Dynamics, Chaos and Complex Systems Group. In 2008, he was elected a Foreign Member of the Lithuanian Academy of Sciences. From August 2010 to January 2011 he was a Visiting Research Professor at Beijing Jiaotong University from the Key Invitation Program for Top-Level Experts of the Chinese Government.



Guanrong Chen (M'87–SM'92–F'97) received the M.Sc. degree in computer science from Zhongshan University, China, in 1981 and the Ph.D. degree in applied mathematics from Texas A&M University, College Station, in 1987. Currently he is a Chair Professor with the Department of Electronic Engineering, City University of Hong Kong, China, and the founding Director of the Centre for Chaos and Complex Networks therein since 2000, prior to which he was a tenured Full Professor with the University of Houston, Houston, TX. His research interests include chaotic dynamics, complex networks, and nonlinear systems control.